Scientia Iranica, Vol. 6, No. 2, pp 149–156

SCIENTIA
IRANICA

Research Note

Upper Bound Analysis of Cylindrical Shells Subjected to Local Loads

G.H. Rahimi[1]

The investigation is concerned with plastic behavior of cylindrical shells, with rectangular attachments well removed from the ends subjected to local radial loads. In the analysis, the upper bound technique is employed to provide the minimum upper bound to the plastic limit load for shell when it is subjected to a local radial load over a rectangular area of the cylindrical shell surface. Furthermore, a two-moment limited interaction yield surface is used. The results are presented for a range of practical geometrical parameters. Alternative collapse mechanism is examined. The limitation of the employed yield surface is also discussed.

INTRODUCTION

In design and analysis of pressure vessels, the problem of externally applied loads has long been of importance to designers and stress analysts. Such loading conditions may occur at nozzles (where they may arise due to reactions of piping system), supports and other attachments. In practice, the analytical methods based on the theory of elasticity are most frequently used in solving this class of problems though many procedures are empirical. Although many elastic formulations have been obtained, probably the most widely used is the shell solution provided by Bijlaard [1-4]. Wichman et al. [5] summarized this work by providing analytical design curves for cylindrical and spherical shells subjected to external loads. However, in pressure vessels with some special conditions, for example nuclear vessels, elasticity solutions are often inadequate. This is particularly true when considering the extremely large loads often defined for emergency and fault conditions. For most of these conditions, an elastic analysis greatly underestimates the load carrying capacity of the vessel. Therefore, for an adequate assessment, an analysis taking into consideration the plastic behavior of the structure must be performed.

Cylindrical pressure vessels invariably have attachments such as supports and branches welded to them. A vessel must be designed in a way that would withstand any local loads which may be transmitted to it through such attachments. The loads may be combinations of normal or shear forces, circumferential or longitudinal bending moments and twisting moments. Here, the analytical bases are concerned with loads being applied over square or rectangular areas of a cylindrical shell. This is because the boundaries of such areas are easier to specify mathematically than, for example, that of a circular area, for which an analysis would be difficult.

The present work is concerned with the plastic behavior of cylindrical vessels when subjected to local radial load through a rectangular attachment.

The upper bound theorem of plasticity has been used by Miller [6] to calculate an upper bound solution for the limit pressure of a sphere with a protruding nozzle, with a partial penetration defect in the sphere running round the junction of the sphere and cylinder. An upper bound to the limit pressure has been determined by considering four independent mechanisms and compared with a lower bound solution in [7] for the same physical situation. In both the upper and lower bound solutions, the two-moment limited interaction yield surface is used. An upper bound analysis for the plastic limit moment of a cylindrical shell subjected to a circumferential bending moment through a square attachment was reported by Kitching et al. [8], along with the experimental behavior of 12 mild steel shells subjected to this type of loading. A similar analysis for cylindrical shells with square attachments subjected to longitudinal moments has been reported by Kitching et al. [9], as well as the experimental behavior of 14 specimens. Both analyses have used a two-moment limited interaction yield surface. These analyses [8,9] have been extended for rectangular attachments by

1. *Department of Mechanical Engineering, Tarbiat Modares University, Tehran, I.R. Iran.*

the author [10] with a modified collapse mechanism. A simple lower bound analysis for a cylindrical shell when it is subjected to local radial load through the rectangular attachments is given in [11].

The experimental and theoretical work on elastic behavior of cylindrical shells subjected to local radial load can be found in more recent literature, for example [12,13], but reports on plastic tests and analyses are rare.

ANALYSIS

The analysis is similar to that of a cylindrical shell subjected to circumferential or longitudinal bending moment [10]. It is simplified by assuming that the principle directions are longitudinal and circumferential. The notation and sign convention for the surface of the attachment along with relevant hinge patterns (eg. hinges are implied at BC, EF, etc) are presented in Figure 1. Due to the symmetry of the problem, it is only necessary to consider the internal energy dissipation of the collapse mechanism viz Regions 1, 2, and 3 of Figure 1c. The direct stresses in all of the plastic regions are compressive. For any point on the shell, the components of displacement in the x, θ and z directions are u, v and w, respectively. It is assumed that $u = 0$ throughout the paper and v and w are small. Strains and curvatures at any point of the middle surface will be given by:

$$e_x = u_{,x} \quad e_\theta = (v_{,\theta} + w)/a \quad 2e_{x\theta} = v_{,x} \quad k_x = -w_{,xx}$$

$$k_\theta = (v_{,\theta} - w_{,\theta\theta})/a^2 \quad 2k_{x\theta} = (v_{,x} - 2w_{,x\theta})/a. \qquad (1)$$

Using $\sigma_\circ$ as the yield stress in simple tension, defining $N_\circ$, $M_\circ$ as $N_\circ = \sigma_\circ t$ and $M_\circ = \sigma_\circ t^2/4$ respectively, where t is the shell thickness, and employing a yield surface with stress resultants provides that:

$$|N_\theta| = N_\circ, \quad |N_{x\theta}| = N_\circ/2,$$

$$|M_\theta| = M_\circ, \quad |M_{x\theta}| = M_\circ/2\ . \qquad (2)$$

N_x and M_x are assumed equal to zero within all regions (but not at the hinges). The energy dissipation within any region is given by:

$$D_i = \int\int_A N_\circ |e_\theta| dx a d\theta + \int\int 2\frac{N_\circ}{2}|e_{x\theta}| dx a d\theta + \int\int M_\circ |k_\theta| dx a d\theta + \int\int 2\frac{M_\circ}{2}|k_{x\theta}| dx a d\theta, \qquad (3)$$

where the limits of the integrals are appropriate for the regions.

The analysis for each of Regions 1, 2 and 3 is now given separately. Here, the different suffixes attached to u, v, w and D will refer to the appropriate region.

Region 1

It is assumed that $u = 0$ and for $c_2 < x < b + c_2$ and $0 < a\theta < c_1$.

$$w_1 = -\gamma(b + c_2 - x), \qquad (4)$$

where $\gamma(= w/b)$ is the angular rotation of Region 1, w is the maximum radial displacement and b indicates the extent of plastic deformation. This formula gives $w_1 = 0$ at hinge BC. Inextensibility is assumed within Region 1 and this gives $e_\theta = 0$ or $v_{,\theta} = -w$ which results in:

$$v_1 = a\theta(b + c_2 - x) + A,$$

but $v_1 = 0$ at hinge BC. Inextensibility is assumed within Region 1 and this gives $A = 0$. Hence, circumference movement will be:

$$v_1 = a\theta(b + c_2 - x). \qquad (5)$$

In this region, one can also write $w_1 \sin\theta + v_1 \cos\theta = 0$, if $0 < \theta < c_1/a << 1$ then $\mathrm{tg}\theta = \theta$, hence, $v_1 = -w_1\theta$. Substituting Equations 4 and 5 into Equation 1 gives:

$$e_x = e_\theta = k_{x\theta} = 0, \quad e_{x\theta} = -\frac{\gamma\theta}{2}$$

$$k_\theta = \frac{\gamma(b + c_2 - x)}{a^2}, \quad k_{x\theta} = -\frac{\gamma\theta}{2a},$$

where rotation at hinges AD and BC is $\gamma = w/b$.

Thus, the total energy expended in Region 1 (and for hinges) after integration is:

$$D_1 = 2M_\circ\gamma c_1 + \frac{N_\circ\gamma b c_1^2}{4a} + \frac{M_\circ\gamma b^2 c_1}{2a^2} + \frac{M_\circ\gamma b c_1^2}{4a^2}\ . \qquad (6)$$

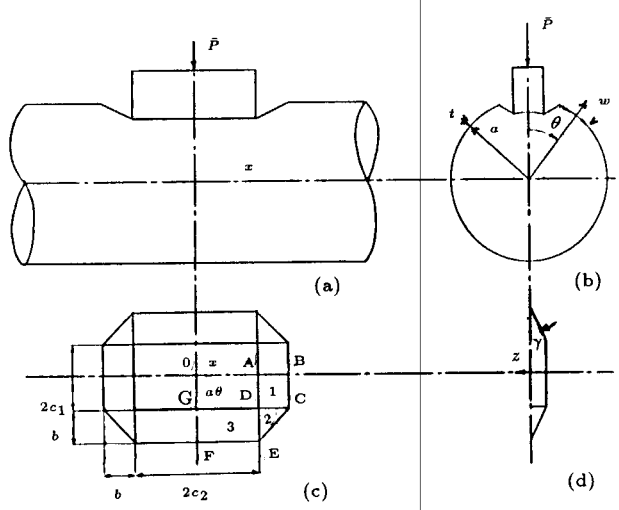

Figure 1. Radial loading.

Region 2

Continuity with Region 1 at $a\theta = c_1$ requires:

$$w_2 = -\gamma((b + c_2 - x) + (c_2 - a\theta)), \tag{7}$$

which gives $w_2 = 0$ along inclined hinge EC, $(x - c_2) + (a\theta - c_1) = b$. It may be shown that:

$$v_2 = \frac{c_1\gamma}{a}((b + c_2 - x) + (c_1 - a\theta)), \tag{8}$$

which can be constructed from the requirements that $v_2 = 0$ along the inclined hinge and $v_2 = v_1$ at $a\theta = c_1$ for continuity with Region 1. Alternatively, if it is assumed that $v_2 = Aw_2$, where A is a constant, by using the continuity condition at the common boundary with Region 1, $A = c_1/a$ and Relation 8 is again derived. Substituting Equations 7 and 8 into Equation 1 gives:

$$e_x = k_x = 0, \quad e_\theta = -\frac{\gamma}{a}(b + c_2 - x + 2c_1 - a\theta),$$

$$e_{x\theta} = -\frac{c_1\gamma}{2a}, \quad k_\theta = -\frac{c_1\gamma}{a^2}, \quad k_{x\theta} = -\frac{c_1\gamma}{2a^2},$$

where rotation at boundary with Region 1 is $\frac{\partial w}{a\partial\theta} = \gamma$, rotation at boundary with Region 3 is $\frac{\partial w}{\partial x} = \gamma$ and rotation at inclined boundary is $\frac{1}{\sqrt{2}}(\frac{\partial w}{a\partial\theta} + \frac{\partial w}{\partial x}) = \frac{2\gamma}{\sqrt{2}}$.

Therefore, the total energy dissipation in Region 2 and for hinges will be:

$$D_2 = 4M_o b\gamma + \frac{3M_o b^2 c_1\gamma}{4a^2} + N_o\gamma(\frac{b^3}{a} + \frac{3b^2c_1}{4a}). \tag{9}$$

It may be noted that the limit of integration along the axial direction can be derived from the geometry of Region 2 which gives:

$$\frac{a\theta - c_1}{b} = \frac{b + c_2 - x}{b} \quad \text{or} \quad x = b + c_1 + c_2 - a\theta.$$

In this region, for example, $e_{x\theta}$, k_θ, $k_{x\theta}$ and e_θ (if $c_1 > b$) are always negative, therefore, the stress resultants have the limit values of $N_\theta = -N_o$, $N_{x\theta} = -N_o/2$, $M_\theta = -M_o$ and $M_{x\theta} = -M_o/2$.

Region 3

Compatibility of the common boundary with Region 2 demands:

$$w_3 = -\gamma(b + c_1 - a\theta), \tag{10}$$

which gives $w_3 = w_2$ at DE. It can also be shown that:

$$v_3 = \frac{\gamma c_1}{a}(b + c_1 - a\theta), \tag{11}$$

which again gives $v_3 = v_2$ at DE, $v_3 = 0$ at FE and $v_3 = b\gamma c_1/a$ at $a\theta = c_1$. Substituting Equations 10 and 11 into Equation 1 gives:

$$e_x = k_x = k_{x\theta} = e_{x\theta} = 0, \quad e_\theta = \frac{-\gamma}{a}(b + 2c_1 - a\theta),$$

$$k_\theta = -\frac{\gamma c_1}{a^2},$$

where rotation at hinges GD and FE is $\gamma = \frac{w}{b}$.

Energy dissipated in Region 3 including that of hinges will be:

$$D_3 = 2M_o\gamma c_2 + \frac{N_o\gamma c_2}{a}(\frac{b^2}{2} + bc_1) + \frac{M_o\gamma c_1 c_2 b}{a^2}. \tag{12}$$

Hence, the total energy dissipation in one quadrant is $D_i = D_1 + D_2 + D_3$. Substituting $M_o = N_o t/4$ into the energy dissipation equation, it is obtained that:

$$D_i = N_o wt(\frac{c_1}{2b} + \frac{c_1^2}{4at} + \frac{c_1^2}{16a^2} + 1 + \frac{5bc_1}{16a^2} + \frac{b^2}{6at} + \frac{3bc_1}{4at} + \frac{c_2}{2b} + \frac{c_1c_2}{4a^2} + \frac{bc_2}{2at} + \frac{c_1c_2}{at}). \tag{13}$$

Now, equating external work done to the energy dissipation in four quadrants, $Pw = 4D_i$. Using the non-dimensional geometric parameters:

$$\Omega = \frac{b}{c_1}, \quad \alpha = \frac{c_1}{c_2}, \quad \gamma = \frac{c_1}{a}, \quad \rho^2 = \frac{c_1^2}{at},$$

provides:

$$P^* = \frac{P}{N_o t} = (4 + \frac{2}{\Omega} + \frac{2}{\alpha\Omega}) + \rho^2(1 + 3\Omega + \frac{2\Omega^2}{3} + \frac{2\Omega}{\alpha} + \frac{4}{\alpha}) + \gamma^2(\frac{1}{4} + \frac{1}{\alpha} + \frac{5\Omega}{4}), \tag{14}$$

where P and P^* are the plastic limit load and non-dimensional limit load, respectively. The terms within the first bracket arise from the work done at the hinges, those within the second bracket from internal work due to direct strains within the regions and those within the third bracket are due to curvature and twist changes within the regions. Parameters α, γ and ρ are given, so that the minimum value of P^* is given by $\frac{\partial P^*}{\partial\Omega} = 0$, or:

$$16\rho^2\alpha\Omega^3 + 3(12\alpha\rho^2 + 8\rho^2 + 5\alpha\gamma^2)\Omega^2 - 24(1 + \alpha) = 0. \tag{15}$$

Solution of the cubic Equation 15 for different values of α and γ gives Ω for the minimum value of P^*.

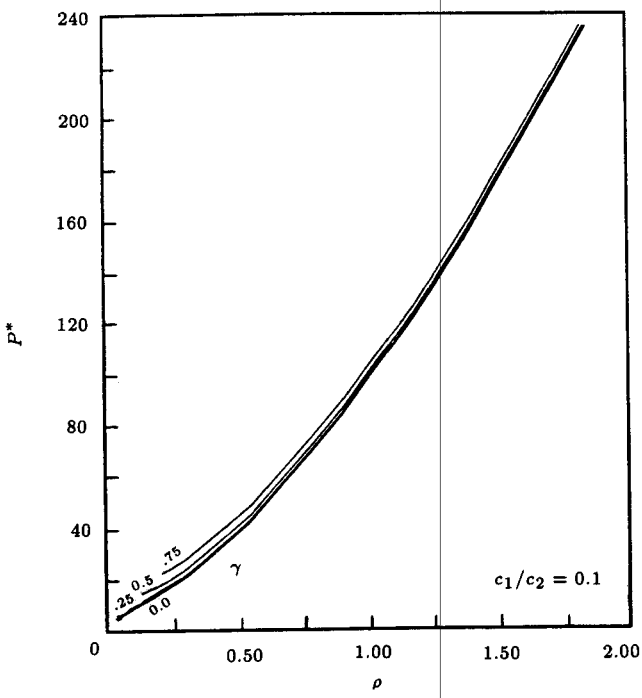

Figure 2a. Limit load versus $\rho(c_1/\sqrt{at})$, for $\alpha(c_1/c_2) = 0.1$.

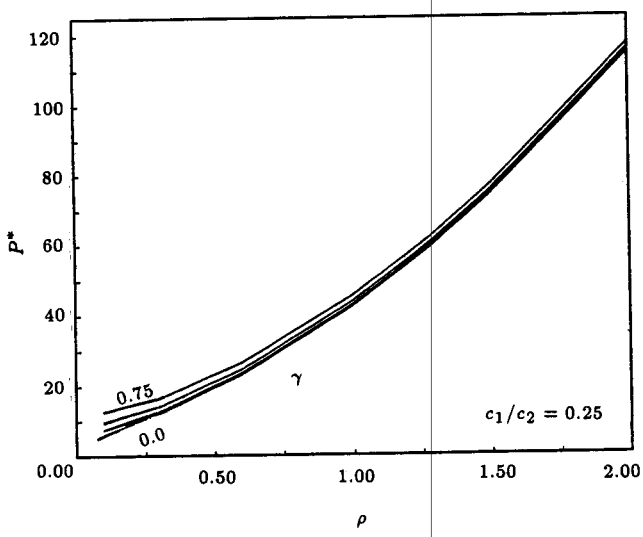

Figure 2b. Limit load versus ρ, for $\alpha = 0.25$.

The solution of Equation 15 for particular values of the parameters α, γ and ρ was obtained by writing a standard computer program.

Figures 2a to 2g demonstrate the curves of minimum P^* against ρ for various values of γ and α. Plastic hinge length parameter Ω and corresponding minimum P^* for various values of ρ, γ and α are given in [10].

ALTERNATIVE COLLAPSE MECHANISM

An alternative collapse mechanism is now examined to see the probable improvement of the limit load.

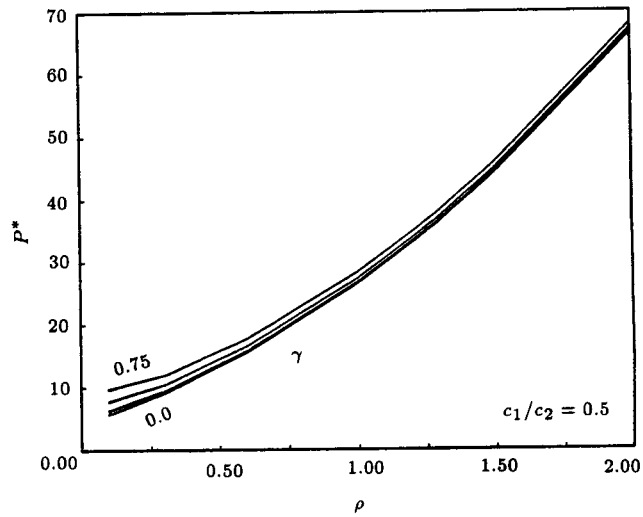

Figure 2c. Limit load versus ρ, for $\alpha = 0.5$.

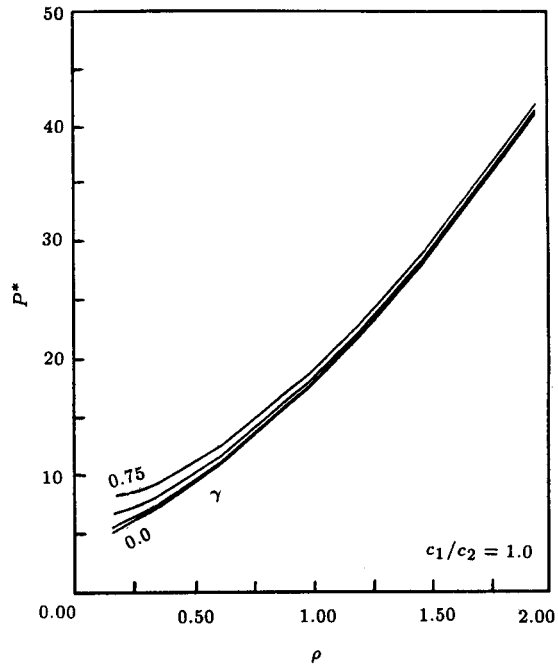

Figure 2d. Limit load versus ρ, for $\alpha = 1.0$.

The hinge pattern is shown in Figure 3, for which the extent of the plastic zone is b in the radial direction and d in the circumferential direction. This involves an extra unknown parameter of that in the analysis of the previous section. Since the same relations and similar procedure of the analysis are employed as before, hence, the details of the calculation are not given here.

Region 1

In this region the velocity field is defined as:

$$w_1 = -\gamma_1(b + c_2 - x) \tag{16}$$

$$v_1 = \gamma_1(b + c_2 - x), \tag{17}$$

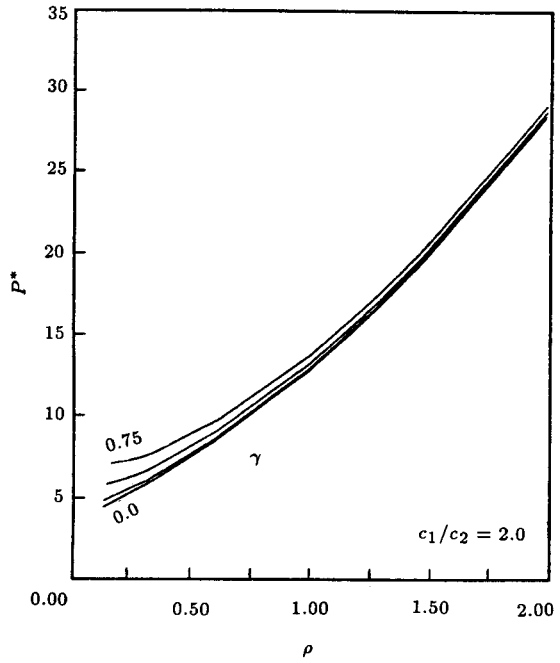

Figure 2e. Limit load versus ρ, for $\alpha = 2.0$.

where $\gamma_1 (= w/b)$ is the rigid body rotation of Region 1. The final expression of energy dissipation in Region 1 is:

$$D_1 = 2M_o\gamma_1 c_1 + \frac{N_o b\gamma_1 c_1^2}{4a} + \frac{M_o\gamma_1 b^2 c_1}{2a^2} + \frac{M_o\gamma_1 b c_1^2}{4a^2}. \quad (18)$$

Region 2

Continuity of common boundary with Region 1 and also $v_2 = w_2 = 0$ at the inclined edge $(x - c_2) = -b(a\theta - c_1)/d + b$ demands:

$$w_2 = -\gamma_1((b + c_2 - x) - \frac{b}{d}(a\theta - c_1)), \quad (19)$$

$$v_2 = \frac{\gamma_1 c_1}{a}((b + c_2 - x) - \frac{b}{d}(a\theta - c_1)). \quad (20)$$

Rotation at common boundary with Region 1 is $\frac{\partial w_2}{a\partial\theta} = \frac{b\gamma_1}{d}$; rotation at common boundary with Region 3 is $\frac{\partial w_2}{\partial x} = \gamma_1$ and rotation at inclined boundary EC is:

$$\frac{b}{\sqrt{b^2 + d^2}}\frac{\partial w_2}{\partial x} + \frac{d}{\sqrt{b^2 + d^2}}\frac{\partial w_2}{a\partial\theta} = \frac{2b\gamma_1}{\sqrt{b^2 + d^2}}.$$

Therefore, the total energy dissipation in Region 2 is:

$$D_2 = 3M_o b_1 + \frac{M_o b^2\gamma_1}{d} + \frac{N_o b\gamma_1}{a}$$
$$(b^2 - \frac{b^2 c_1^2}{d^2} - \frac{b^3}{d} - \frac{b^3 c_1}{d^2} + \frac{bc_2}{2} + \frac{3bc_1}{2}$$
$$+ c_1 c_2 + \frac{b^4}{6d^2} + \frac{bc_1^2}{d} + \frac{b^2 c_1}{4d} - \frac{b^2 c_2}{2d} - \frac{bc_1 c_2}{d})$$
$$+ \frac{M_o\gamma_1 bc_1}{a^2 d}(b^2 - \frac{b^3}{2d}) + \frac{M_o\gamma_1 c_1 b^2}{2a^2}(1 - \frac{b}{2d}). \quad (21)$$

Region 3

Compatibility at common boundary with Region 2 requires $w_3 = w_2$ and $v_2 = v_3$ at $x = c_2$, hence:

$$w_3 = -\gamma_2(d + c_1 - a\theta), \quad (22)$$

$$v_3 = -\frac{\gamma_2 c_1}{a}(d + c_1 - a\theta), \quad (23)$$

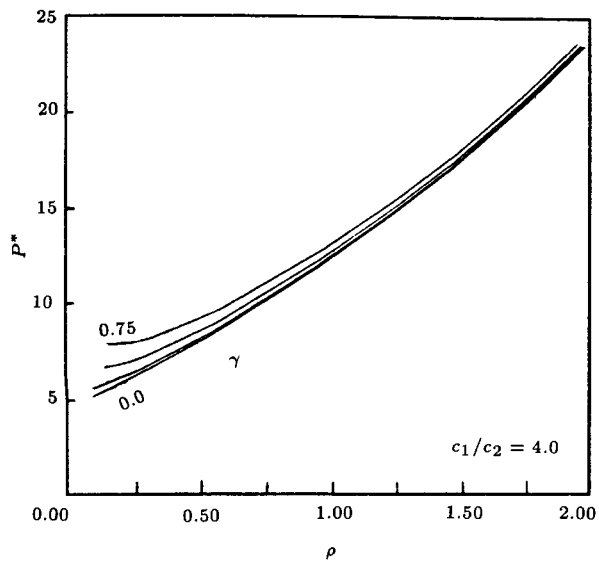

Figure 2f. Limit load versus ρ, for $\alpha = 4.0$.

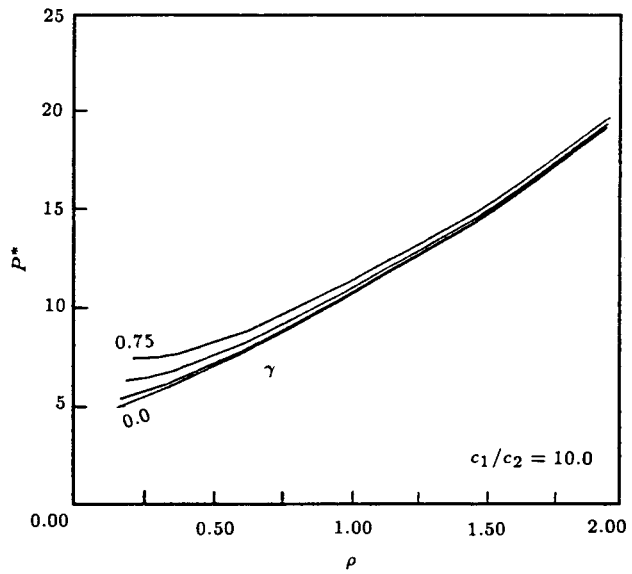

Figure 2g. Limit load versus ρ, for $\alpha = 10.0$.

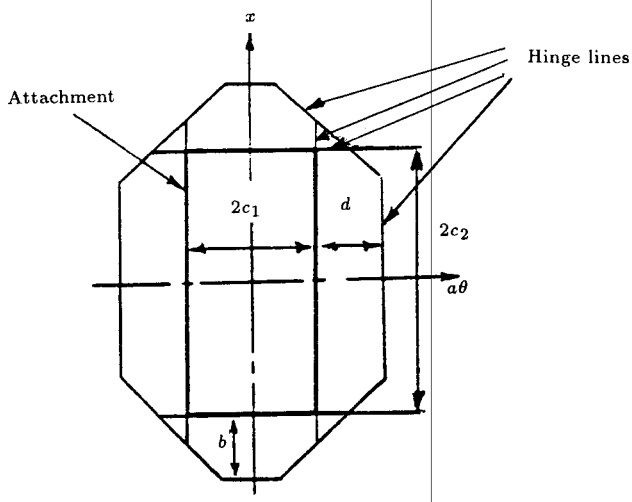

Figure 3. Alternative hinge pattern.

where $\gamma_2(= w/d)$ is the rigid body rotation of Region 3. Rotation at GD and FE are $\gamma_2 = w/d$. Total energy dissipation in Region 3 will be:

$$D_3 = M_o\gamma_2 c_2 + M_o\gamma_2 c_2 + \frac{N_o\gamma_2 c_2 b}{a}$$

$$(d + c_1 - \frac{b}{2}) + \frac{M_o\gamma_2 b c_1 c_2}{d}. \qquad (24)$$

Therefore, the total energy dissipation in one quadrant is $D_i = D_1 + D_2 + D_3$. Substituting $M_o = \sigma_o t^2/4$ and $N_o = \sigma_o t$ into D_i equation and equating the total energy dissipation in four quadrants to the external work done ($D_e = Pw$) gives the appropriate balance equation.

Using the non-dimensional geometric parameters:

$$\Omega_1 = \frac{b}{c_1},\ \Omega_2 = \frac{d}{c_1},\ \alpha = \frac{c_1}{c_2},\ \gamma = \frac{c_1}{a},\ \rho^2 = \frac{c_1^2}{at},$$

yields:

$$P^* = (3 + \frac{2}{\Omega_1} + \frac{\Omega_1}{\Omega_2} + \frac{2}{\alpha\Omega_2}) + \rho^2(1 + 4\Omega_1^2$$

$$+ 6\Omega_1 + \frac{4}{\alpha} - \frac{4\Omega_1^2}{\Omega_2^2} - \frac{4\Omega_1^3}{\Omega_2^2} - \frac{4\Omega_1^3}{\Omega_2} + \frac{6\Omega_1}{\alpha}$$

$$+ \frac{2\Omega_1^4}{3\Omega_2^2} + \frac{4\Omega_1}{\Omega_2} + \frac{\Omega_1^2}{\Omega_2} - \frac{4\Omega_1^2}{\alpha\Omega_2})$$

$$+ \gamma^2(\frac{1}{4} + \Omega_1 + \frac{\Omega_1}{\alpha\Omega_2} - \frac{\Omega_1^3}{2\Omega_2^2} + \frac{3\Omega_1^2}{4\Omega_2}). \qquad (25)$$

Values of α, γ and ρ are given and the minimum values of P^* occur at a point where the first derivatives of P^* with respect to Ω_1 and Ω_2 simultaneously vanish [14]:

$$\frac{\partial P^*}{\partial \Omega_1} = 0 \quad \text{and} \quad \frac{\partial P^*}{\partial \Omega_2} = 0\,. \qquad (26)$$

Solving this system of nonlinear equations requires the application of a linearization technique. Several classical procedures for solving such systems exist. A typical procedure is Newton-Raphson method, which is chosen here. A computer program is written for finding the upper bound plastic extent parameters Ω_1 and Ω_2 corresponding to minimum P^* for certain values of parameters $\alpha(= 0.25)$, $\gamma(= 0)$ and $\rho(= 0.2$ to $2.0)$, which are tabulated in Table 1. Table 1 also shows the corresponding values of Ω and P^* calculated according to the analysis of the previous sections ($\Omega_1 = \Omega_2 = \Omega$).

DISCUSSION OF RESULTS

The upper bound of the non-dimensional limit radial load for an open-ended cylindrical shell is plotted in Figure 2 against the parameter $\rho(= c_1/\sqrt{at})$ for various values of $\gamma(= c_1/a)$ and $\alpha(= c_1/c_2)$. The results have been computed using Equation 14. It has been assumed that the cylindrical shell is long enough for the influence of the ends to be neglected. The theoretical work indicates that when the shell is subjected to a local load, only a small local region consequently becomes plastic. The position $\theta = (b + c_1)/a$ in the circumferential direction (and also $x = b + c_2$ in the axial direction) of the boundary, separating the plastic from the rigid region is one of the unknowns of the problem.

The most significant results of the analysis are outlined as follows:

1. Figure 2 suggests that there is a continuous and consistent relationship between applied load and ρ. The figure also indicates that as parameter ρ becomes greater the value of the corresponding limit load increases.
2. For many practical situations, γ^2 is small enough to make the third term in Equation 14 negligible. The resulting values of P^* will still become upper bound to the limit load. Of course, it appears that neglecting energy dissipation due to loading within the plastic zones, provides results only marginally different from those with $\gamma \neq 0$. Neglecting γ for simplifying calculations is of the same order as ignoring bending strain energy within the Regions . Figure 2 illustrates that for each fixed value of α, the change of γ has little effect on the limit load, though as γ rises, the limit load increases a little. The influence of γ becomes smaller as ρ increases and sometimes the curves are coincident for the range of γ investigated.
3. For high values of α (i.e. 2, 4 and 10), increase of ρ has less effect on the increase of the limit load. This means that as α rises the slope of the curves decreases. The reason is thought to be that when the circumferential dimension is small, a higher load

Table 1. Comparison of results of different collapse mechanisms.

ρ	Results of the Alternative Collapse Mechanism ($\alpha = 0.25$)			Results of the Assumed Mechanism ($b = d$)	
	$\Omega_1 = \frac{b}{c_1}$	$\Omega_2 = \frac{d}{c_1}$	P^*	$\Omega = \frac{b}{c_1}$	P^*
0.2	3.46	10.86	9.708	3.92	9.37
0.3	2.139	6.493	12.981	2.752	12.342
0.37	1.747	4.944	15.472	2.25	14.83
0.6	1.085	2.615	24.848	1.464	23.262
1.0	0.645	1.342	46.127	0.905	42.55
1.23	0.511	1.011	61.422	0.731	57.363
1.5	0.422	0.807	79.508	0.613	74.298
2.0	0.311	0.571	122.413	0.464	114.541

is required in order for the surface to be deformed plastically.

4. Results also indicate that the value of Ω (non-dimensional extent of the plastic region) associated with the non-dimensional limit radial loads for small values of ρ (say 0.1) are almost indentical.

5. Comparison between the results (Table 1) of the two collapse mechanisms shows that the minimum values of P^* are almost indentical, although the plastic extent in each of the longitudinal and circumferential directions is different in magnitude. This indicates that the minimum values of P^*, which are based on the analysis of the previous section, have been improved only marginally. However, a better view regarding the extent of the plastic zone in each of the axial and hoop directions may be achieved by considering the collapse mechanism, which is suggested previously.

6. As an example, for a specific cylindrical shell, with the following geometrical dimensions $a = 52.64$ mm (2.0725 in), $t = 1.4$ mm (0.055 in) , $2c_1 = 6.35$ mm (0.25 in), $2c_2 = 25.4$ mm (1 in), non-dimensional parameters will be $\alpha = 0.25$, $\rho^2 = 0.137$, $\gamma = 0.0619$. Cubic Equation 15 gives $\Omega = 2.25$, so extent of plastic deformation will be $b = 7.143$ mm (0.281 in). From Table 1, non-dimensional radial limit load is $P^* = 14.83$. Hence, for a typical yield stress, say $\sigma_o = 103.42$ Mpa (15 ksi), Equation 14 gives $P = 103.42 \times 1.4^2 \times 14.83 = 3$ kN (673 lb) .

7. Using two-moment limited interaction yield surface needs some modification for calculating the plastic limit loads. This point will be explained in the appendix.

ACKNOWLEDGEMENT

The author is indebted to Prof. R. Kitching for his invaluable advice and guidance given throughout the duration of this research program.

REFERENCES

1. Bijlaard, P.P. "Stresses from radial loads in cylindrical pressure vessels", *Welding J. Research Supplement*, **33**, pp 15-23 (1954).
2. Bijlaard, P.P. "Stresses from local loading in cylindrical pressure vessels", *Trans. ASME*, **77**, pp 805-816 (1955).
3. Bijlaard, P.P. "Stresses from radial loads and external moments in cylindrical pressure vessels", *Welding J. Research Supplement*, pp 608-23 (1955).
4. Bijlaard, P.P. "Additional data on stresses in cylindrical shells under local loading", *Welding Research Council Bulletin*, **50** (1959).
5. Witchman, K.R., Hopper, A.G. and Mershon, J.L. "Local stresses in spherical and cylindrical shells due to external loadings", *Welding Research Council Bulletin*, **107** (1980).
6. Miller, A.G. "Upper bound limit analysis of spherical vessels with protruding nozzles and associated defects at the intersection", CEGB, RD/B/ 5117 N 81 (1981).
7. Goodal, I.W. and Miller, A.G. "Limit analysis of pressure vessels with protruding nozzles and associated defects", CEGB, RD/B/ 5038 N 81 (1981).
8. Kitching, R., Hughes, J.F. and Jones, N. "Limit loading of cylindrical shells subjected to local circumferential bending moments", *Int. J. Mech. Sci.*, **20**, pp 61-81 (1978).
9. Kitching, R., Hussein, D. and Jones, N. "Limit loads for cylindrical shells subjected to local longitudinal bending moments", *Int. J. Mech. Sci.*, **24**, pp 673-90 (1982).
10. Rahimi, G.H. "Plastic limit analysis of cylindrical shells subjected to local loads through rectangular attachment", M.S. Dissertation, University of Manchester (1986).
11. Rahimi, G.H. "Lower bound analysis of cylindrical shells subjected to local radial load", Amir Kabir J., Amir Kabir University, Tehran, Iran (in Perssian) (1988).
12. Findlay, G.E. and Timmins, W. "Local radial loads on cylinders: BS 5500 predictions versus experimental results", *Int. J. Pres. Ves. & Piping*, pp 33-48 (1987).

13. Tooth, A.S. and Motashar, F.A. "Radial loading of a cylindrical vessel through a rectangular rigid attachment", *Int. J. Pres. Ves. & Piping*, **37**, pp 345-63 (1989).

14. Simons, D.M., *Non Linear Programming for Operations Research*, Prentice-Hall Inc. (1960).

15. Hodge, P.G. Jr "Yield conditions for rotationally symmetric shells under axi-symmetric loading", *J. Appl. Mech.*, pp 323-331 (1960).

16. Gill, S.S. "The limit pressure for a flush cylindrical nozzle in a spherical pressure vessel", *Int. J. Mech. Sci.*, **6**, pp 105-115 (1964).

17. Ellyin, F. "The effect of yield surfaces on the limit pressure of intersecting shells", *Int. J. Solids & Structures*, **5**, pp 713-25 (1969).

18. Onat, E.T. and Prager, W. "Limit analysis of shells of revolution", *Proc. Roy, Netherland Acad. Sci.*, pp 534-548 (1954).

19. Robinson, M. "A comparison of yield surfaces for thin shells", *Int. J. Mech. Sci.*, **13**, pp 345-54 (1971).

APPENDIX

Discussion on Yield Surface

Generally, the results of a 2-moment limited interaction yield surface is a four-dimensional surface defined by twelve planes. Generally, using this yield condition needs some modification in calculating the limit load. For example, it can be shown that this yield surface reduced by a scale factor 0.618 is entirely within the true interaction surface for a shell made of material, which follows Tresca yield criterion [15]. Thus, the true load of a shell for Tresca yield conditions is between 0.618 and 1 times the plastic collapse load calculated using the limited interaction surface. Therefore, the upper bounds calculated for this approximate yield surface are also upper bounds for Tresca yield surface. Experimental evidence exists which indicates that the approximation of using a 2-moment limited interaction surface is quite reasonable in most practical circumstances (e.g. [16]). However, a theoretical comparison of the limit pressure obtained with 2-limited moment surfaces has been made by Ellyin [17], who shows that the approximation can be quite inaccurate for certain extreme geometries. Now, the employed yield surface is examined in more detail.

Approximation to the Tresca Yield Condition

Based on conclusions reached by Onat and Prager [18], if all bending behavior except at the hinges is neglected (i.e. $\gamma = 0$) and all shear force effects are also ignored, it can be readily shown that for all plastic zones and hinges (except at inclined hinges) and for all cases of loading, a yield stress of 0.618 $\sigma_\circ$ (i.e., a reduction factor of 0.618) would still give an upper bound since the yield surface still circumscribes or touches the exact one. Therefore, by introducing this reduction factor to the evaluated limit radial load for certain geometries of the shell and attachment, one can get an improved limit load $P = 1.854$ kN which is still upper bound to the limit load.

Approximation to the Mises Yield Condition

In this case, there is no need to neglect bending behavior and shear forces, therefore, it is possible to obtain a better yield surface than Tresca approximation and, hence, an improved upper bound limit load. The following Equation [19]:

$$(n_x^2 - n_x n_\theta + n_\theta^2 + 3n_{x\theta}^2) + (m_x^2 - m_x m_\theta + m_\theta^2 + 3m_{x\theta}^2) = 1, \quad \text{(A1)}$$

can be used to obtain a reduction factor corresponding to this yield condition ($n_x = N_x/N_\circ, m_x = M_x/M_\circ$, etc.). For this purpose, the yield surface is examined for longitudinal bending moment of each region. It can be noted that signs of the generalized stresses do not alter the yield condition.

Region 1

In the interior zone, $N_{x\theta} = -\frac{N_\circ}{2}, M_{x\theta} = \frac{M_\circ}{2}, M_\theta = M_\circ$. If it is assumed that $\frac{N}{N_\circ} = \frac{M}{M_\circ} = K, \frac{3}{4}K^2 + K^2 + \frac{3}{4}K^2 = 1$ is obtained giving $5K^2 = 1$, so $K = 0.632$. At the hinge AD, $N_{x\theta} = -\frac{N_\circ}{2}, M_{x\theta} = \frac{M_\circ}{2}, M_x = -M_\circ$ and $M_\theta = M_\circ$, therefore, $\frac{3}{4}K^2 + K^2 - K^2 + K^2 + \frac{3}{4}K^2 = 1$ so $K = 0.632$. At hinge BC, $N_{x\theta} = -\frac{N_\circ}{2}$, $M_{x\theta} = \frac{M_\circ}{2}$, $M_x = M_\circ$ and $M_\theta = M_\circ$, again $K = 0.632$ is obtained.

Region 2

Within the plastic zone, $N_\theta = -N_\circ, N_{x\theta} = \frac{-N_\circ}{2}, M_\theta = -M_\circ$ and $M_{x\theta} = -\frac{M_\circ}{2}$. Hence, $K = 0.534$. At the hinge DE, following the same procedure gives $K = 0.532$ and at the hinge DC, $K = 0.534$. At the inclined hinges by assuming $M_\theta = M_x = \frac{M_\circ}{\sqrt{2}}$, $K = 0.557$ is obtained. The same results are derived for Region 3. Therefore, when $\sigma_\circ$ is replaced by 0.632 $\sigma_\circ$, a circumscribing yield surface is obtained at all conditions considered. A reduction factor of 0.756 is suggested in [9] which leads to an improved upper bound and results in a longitudinal bending moment M^* values for the upper bound curve being reduced by an average of 13%. The same procedure can be carried out for hoop moment [8]. If the same analysis is followed for radial load, a factor of 0.707 will still give an upper bound since the yield surface still circumscribes or touches the exact one. In this case, for a typical cylinder considered previously, $P = 2.121$ kN is obtained.